

Important declarations

Please remove this info from manuscript text if it is also present there.

Associated Data

New DNA/RNA/peptide etc. sequences were reported.

Sequences supplied by author here:

The new species sequence added here is accessible via GenBank accession numbers OQ922018. The newly obtained previously unpublished sequences cited are accessible via GenBank accession numbers OR588066 and OR588068

Data supplied by the author:

Holotype: <https://www.morphosource.org/concern/media/000570594?locale=en> Paratype:
<https://www.morphosource.org/concern/media/000570600?locale=en>

Required Statements

Competing Interest statement:

The authors declare that they have no competing interests.

Funding statement:

Participation by BWF was supported by the SIO Director's Office, the Scripps Oceanographic Collections Fund, and the Lehman-Kennel Endowment for the Collections at SIO. The Natural History Museum of Los Angeles County supported the expedition. Funding from the National Science Foundation supported the μ CT scanner at the NHMLA (DBI 2215184).

***Halichoeres sanchezi* n. sp., a new wrasse from the Revillagigedo Archipelago of Mexico, tropical eastern Pacific Ocean (Teleostei: Labridae)**

Benjamin C Victor ^{Corresp., 1, 2}, Benjamin W Frable ³, William B Lucht ⁴

¹ Guy Harvey Research Institute, Nova Southeastern University, Dania Beach, Florida, United States

² Marine Biology, Ocean Science Foundation, Irvine, California, United States

³ Marine Vertebrate Collection, Scripps Institution of Oceanography, La Jolla, California, United States

⁴ Ichthyology, Natural History Museum of Los Angeles County, Los Angeles, California, United States

Corresponding Author:

Benjamin C Victor^{1, 2}

Email address: ben@coralreeffish.com

12 Abstract

A new labrid fish species, *Halichoeres sanchezi* n. sp., is described from eight specimens collected in the Revillagigedo Archipelago in the tropical eastern Pacific Ocean, off the coast of Mexico. The new species belongs to the *Halichoeres melanotis* species complex that is found throughout the region, differing in 2.4% in the mtDNA cytochrome c oxidase I sequence from its nearest relative, *H. melanotis* from Panama, and 2.9% from *Halichoeres salmofasciatus* from Cocos Island, off Costa Rica. The complex is distinguished from others in the region by having a black spot on the opercular flap and a prominent black area on the caudal fin of males. The juveniles and initial phase of the new species closely resemble those of *H. salmofasciatus* and *Halichoeres malpelo* from Malpelo Island of Colombia, differing in having an oblong black spot with a yellow dorsal margin on the mid-dorsal fin of initial-phase adults as well as on juveniles. In contrast, the terminal-phase male color pattern is distinct from other relatives, being vermilion to orangish brown with dark scale outlines, a white patch on the upper abdomen, and a prominent black band covering the posterior caudal peduncle and base of the caudal fin. The new species adds to the list of endemic fish species for the isolated archipelago and is an interesting case of island endemism in the region. The discovery was made during the joint 2022 collecting expedition to the archipelago, which featured a pioneering collaborative approach to an inventory of an island ichthyofauna, specifically including expert underwater photographers systematically documenting specimens in situ before hand-collection, and then photographed fresh, tissue-sampled, and subsequently vouchered in museum collections.

Deleted: and it diverges

13 Introduction

14 The geography of the tropical eastern Pacific Ocean (TEP) provides a useful proving ground for
15 answering questions about marine island biogeography. There is a long and relatively linear
16 coastline with a narrow continental shelf and a series of isolated offshore islands. Unlike most
17 other tropical marine regions, each island group contains a different set of the regional shorefish
18 fauna (Allen & Robertson, 1994) and the patterns of occurrence, especially the prevalence of

19 endemism and degrees of connectivity, can be directly assessed and hypotheses can be tested.

20 The Revillagigedo Archipelago of Mexico, forming the Reserva de la Biosfera Archipelago de

21 Revillagigedo, includes the islands of Clarion, Socorro, San Benedicto, and Roca Partida, and is

22 about 400 km south of the Baja California peninsula and about 700 km west of Manzanillo. It is

23 one of the more remote and least visited of the island groups of the TEP, with a short history of

24 collecting expeditions and a very limited number of museum collections, especially compared to

25 more well-surveyed TEP islands, such as the Galapagos Archipelago.

26 In November 2022, a joint expedition formed by an international team of ichthyologists and a
 27 cadre of experienced underwater photographers, visited the four islands of the archipelago and
 28 compiled a comprehensive inventory of the shallow shorefish fauna, with in situ photographic
 29 documentation of all of the fish species encountered. All species collected were sampled for
 30 tissues and subsequently DNA-barcoded, i.e. sequenced for the mtDNA cytochrome c oxidase I
 31 gene (COI). One of the more compelling aspects of the expedition was the contemporaneous
 32 underwater documentation, including on digital video, of the discovery and collection of the
 33 holotype of a new species of fish, in this case a new labrid species of the large genus *Halichoeres*
 34 Ruppell, 1835.

35 The new species is the local representative of the widespread TEP *Halichoeres melanotis* (Gilbert, 1890)
 species

36 complex, comprising *H. melanotis* along the mainland,

Deleted: which is made up of

37 *Halichoeres salmofasciatus* Allen & Robertson, 2002, endemic to Cocos Island, and *Halichoeres*
 38 *malpelo* Allen & Robertson, 1992, endemic to Malpelo Island (Robertson & Allen, 2015). The
 39 new species was not listed in recent species lists for the Revillagigedo Archipelago (Del Moral-Flores, Gracian-
 Negrete & Guzman-Camacho, 2016; Fourriere et al. 2016). It had been photographed at least once previously,
 but had not been identified with any
 40 certainty. It is a particularly elusive wrasse, with adults difficult to approach, accounting for the
 41 dearth of documentation despite many tourist divers photographing fishes in the archipelago. We
 42 collected a series of specimens on San Benedicto, the northernmost island of the
 43 Revillagigedo Archipelago (Fig. 1).

44 Materials & Methods

45 Specimens of the new species are accessioned in the Coleccion Nacional de Peces at
 46 the Universidad Nacional Autonoma de Mexico (CNP-IBUNAM), the Natural History Museum
 47 of Los Angeles County (LACM), and the Marine Vertebrate Collection of Scripps Institution of

48 Oceanography (SIO). Permits for the travel, boats, collection, and export were issued to the
 49 Universidad Nacional Autónoma de México by the Secretariat of Agriculture, Livestock, Rural
 50 Development, Fisheries and Food (SAGARPA) of the Federal Government of Mexico (permit
 51 number PPF/DGOPA-A-099/22). Measurements and counts of congeners used for comparative
 52 purposes were from specimens housed at LACM, SIO, and the NMNH or values taken from the
 53 literature (Allen & Robertson, 1992; 1994; 2002; Robertson & Allen, 2015).

54 Measurements were taken as previously described in Victor (2016). Specifically, the length of specimens is
 given as standard length (SL), measured from the median anterior end
 55 of the upper lip to the base of the caudal fin (posterior end of the hypural plate); body depth is
 56 the greatest depth from the base of the dorsal-fin spines to the ventral edge of the abdomen
 57 (correcting for any malformation of preservation); body width is measured just posterior to the
 58 gill opening; head length from the front of the upper lip to the posterior end of the opercular flap;
 59 orbit diameter is the greatest fleshy diameter of the orbital rim, and interorbital width the least
 60 bony width between the orbits; snout length is measured from the median anterior point of the
 61 upper lip to the nearest fleshy rim of the orbit; caudal-peduncle depth is the least depth, and
 62 caudal-peduncle length the horizontal distance between verticals at the rear base of the anal fin
 63 and the caudal-fin base; predorsal, prepelvic and preanal lengths are oblique measurements taken
 64 from the median anterior point of the upper lip to the base of the first spine of each respective
 65 fin; lengths of spines and rays are measured to their extreme bases; caudal-fin and pectoral-fin
 66 lengths are the length of the longest ray; pelvic-fin length is measured from the base of the pelvic
 67 spine to the tip of the longest soft ray. The upper rudimentary pectoral-fin ray is included in the
 68 count. Lateral-line scale counts list the last pored scale that overlaps the end of the hypural plate
 69 as +1. The count of gill rakers is made on the first gill arch and includes all rudiments.

70 Proportional measurements were taken with digital calipers or from radiograph images using
 71 ImageJ (<https://imagej.net/>) and are rounded to the nearest 0.1. Counts were taken from
 72 specimens, digital radiographs, and micro-computer tomography (microCT) scans. Counts and
 73 measurements for the paratypes are shown in parentheses following data for the holotype (some
 counts and measurements were not made on the juvenile paratype CNP-IBUNAM 23979).

74 Proportional morphological measurements as percentages of the standard length are presented in
 75 Table 1 and proportional morphological measurements in the diagnosis and description are presented as the number
 of times in SL, HL, or body depth.

76 Fluorescent emission was documented using a Canon 5D Mark IV DSLR camera with a Canon
 77 EF 100mm f/2.8L Macro IS USM lens. Photographs were taken using two NightSea Xite
 78 Fluorescent Flashlights that emitted royal blue light (ca 440-460nm). Each light was held at
 79 approximately 45° to the subject and was equipped with a 15° diffuser cap. A 500nm Tiffen #12
 80 Yellow Filter was placed in front of the lens for all photographs. Micro-computed tomography
 81 (μCT) scans were used to visualize internal skeletal anatomy. Scans were performed at the
 82 NHMLA on a Bruker Skyscan 1273. Scans of the holotype and one of the paratypes were
 83 conducted with and without a 1mm aluminum filter, with 70-90kV, 166-214μA, 471-636ms
 84 exposure times, with a 10-34μm voxel size. All scans were reconstructed using the software
 85 NRecon v2.2.0.6 (Bruker) and visualized using CTVox (Bruker). CT scans were uploaded to
 86 Morphosource.org for the holotype
 87 <https://www.morphosource.org/concern/media/000570594?locale=en>
 88 and the largest paratype
 89 <https://www.morphosource.org/concern/media/000570600?locale=en>

90 A sample of muscle tissue was taken from the holotype, preserved in 90% ethanol and maintained at room
 temperature until sequencing. Standard DNA extractions, primers, and sequencing protocols followed those
 described in Victor, Alfaro & Sorenson (2013). Specimen information and barcode-sequence data from this
 study were compiled using the

Deleted: as

91 Barcode of Life Data Systems (BOLD) (Ratnasingham & Hebert, 2007) and all sequences are publicly
 92 accessible on BOLD and
 93 GenBank. Sequence divergences were calculated using BOLD
 94 with the Kimura 2-parameter (K2P) model. Genetic
 95 distances were calculated by the BOLD algorithm, both as uncorrected p-distances and as K2P
 distances.

The COI sequence for the new species was compared to other members of the *H. melanotis* species complex as well as to the remaining New World *Halichoeres* species [where publicly available](#). The genus is well covered in both the TEP and western Atlantic, with almost all species presently sequenced for COI. The unrelated Indo-Pacific species *Halichoeres argus* (Bloch & Schneider, 1801) was selected as an outgroup. A consensus neighbor-joining phylogenetic tree was constructed in Geneious Prime v2023.2.1 using the Tamura-Nei genetic distance model and 100 bootstrap replicates.

96 The electronic version of this article in Portable Document Format (PDF) will represent a
 97 published work according to the International Commission on Zoological Nomenclature (ICZN),
 98 and hence the new names contained in the electronic version are effectively published under that
 99 Code from the electronic edition alone. This published work and the nomenclatural acts it
 100 contains have been registered in ZooBank, the online registration system for the ICZN. The
 101 ZooBank LSIDs (Life Science Identifiers) can be resolved and the associated information viewed

102 through any standard web browser by appending the LSID to the prefix <http://zoobank.org/>. The
103 LSID for this publication is urn:lsid:zoobank.org:pub:0FF79EE8-EB5A-45B3-98CE-
104 9A420881DAA0. The online version of this work is archived and available from the following
105 digital repositories: PeerJ, PubMed Central SCIE and CLOCKSS.

141
142 *Halichoeres sanchezi* n. sp. urn:lsid:zoobank.org:act:608591F4-2A1B-4271-9BB2-
143 0F0B2BD2DC4E

144 Tailspot Wrasse, Doncella Colimanchada (Spanish)

145 mtDNA COI sequence BIN <https://doi.org/10.5883/BOLD:AFA9780>

146

147 Figures 2-6, Table 1.

148

149 **Holotype.** LACM 61379, 123.1 mm SL, Mexico, Colima, Revillagigedo Archipelago, San
150 Benedicto Island, canyon rubble plain site, sta. WBL 275, 19°17.740' N, 110°48.466' W
151 (19.2957, -110.8078); 21-22 m depth; spear, W.B. Ludt, 30 November 2022.

152 **Paratypes.** (7 specimens 32.3-53.3 mm SL), CNP-IBUNAM 23979, 39.1 mm SL, sta. WBL
153 274, same locality as holotype, quinaldine and handnet, B.W. Frable, 30 November 2022; CNP-
154 IBUNAM 23979, 2, 19.8-32.3 mm SL, sta. WBL 274, same locality as holotype, quinaldine and
155 handnet, C.A. Sanchez et al., 30 November 2022; LACM 61380, 53.3 mm SL, sta. WBL 274,
156 same locality as holotype; quinaldine and handnet, B.W. Frable, 30 November 2022; SIO 23-48,
157 40.4 mm SL, sta. WBL 279, 19°17.795'N, 110°48.351'W, quinaldine and handnet, C.A. Sanchez,
158 30 November 2022; SIO 23-50, 46.2 mm SL, sta. WBL 274, same locality as holotype,

159 quinaldine and handnet, C.A. Sanchez et al., 30 November 2022; SIO 23-51, 36.5 mm SL, sta.

160 WBL 275, same locality as holotype; quinaldine and handnet, B.W. Frable, 30 November 202.

161 **Diagnosis.** Dorsal-fin rays IX,12; anal-fin rays III,12; pectoral-fin rays 13; lateral-line pored scales 26 (+1 on
caudal-fin base); suborbital pores 6; gill rakers

162 14-16; a pair of large, projecting, and slightly recurved canine teeth anteriorly in each jaw, the

163 lowers curving forward and fitting between uppers when mouth closed, a second pair of canines

164 about half size of first, followed by rows of mostly caniniform teeth, no canine posteriorly at

165 corner of mouth; body elongate, depth 3.6-4.2 in SL; body width 2.2-3.0 in depth; caudal

166 fin slightly rounded; TP vermilion on head to orangish-brown on body, yellow-cream ventrally with a dark
cross-

167 hatch pattern outlining scales, opercular flap diffusely dark and purple; a prominent large black

168 blotch covering rear caudal peduncle and proximal half of caudal fin, a pale patch over mid-

169 abdominal area underlying pectoral fin; a small black spot on first dorsal-fin membrane; IP and

170 juvenile fish grey ventrally becoming yellowish posteriorly with a broad midlateral red band from snout to

171 caudal peduncle, often breaking up into horizontal block segments, including a distinct black

172 crescent or oval spot on expanded soft flap of upper operculum, and ending in a horizontal

173 oblong black spot at caudal-fin base; a similar narrower band runs along upper body below base

174 of dorsal fin from snout to upper caudal peduncle; fins clear except for a large oblong black

175 spot, edged in yellow dorsally, centered over membranes of last dorsal-fin spine and first three

176 rays and extending partially onto upper body (present in both juvenile and IP adults).

177 **Description.** Dorsal-fin rays IX,12; anal-fin rays III,12, all soft dorsal and anal-fin segmented

178 rays branched, last split to base; pectoral-fin rays 13, first rudimentary, second unbranched, all remaining rays
branched;

179 pelvic-fin rays I,5; principal caudal-fin rays 6 + 6, upper

Deleted: (counting uppermost rudimentary ray)

Formatted: Space Before: 0 pt

Deleted: -

Deleted: -

Deleted: -

Deleted: 6+6

Deleted: 6

180

procurrent rays 6, anteriormost four unsegmented, remaining rays segmented; lower procurrent rays 6
anteriormost four unsegmented, remaining rays segmented; pored lateral-line scales 26 (+1 on caudal-fin
base); gill rakers 14

Deleted: and 6
Deleted: (each with 4 unsegmented)

181

(14-16); branchiostegal rays 5; vertebrae 10 + 15.

Deleted: -

182

Body elongate and compressed, depth 3.6 (3.8-4.2) in SL, body width 8.9 (8.9-10.8) in SL,

Deleted: -
Deleted: , and compressed

183

2.5 (2.2-2.8) in depth; head length 3.3 (3.0-3.2) in SL; snout pointed and short, its length 3.5

Deleted: -

184

(3.5-4.1) in HL; orbit diameter 5.5 (4.1-4.9) in HL; interorbital space broadly convex, least bony

Deleted: and

185

width 5.2 (5.6-7.9) in HL; caudal peduncle short and narrow, least depth 2.2 (2.3-2.5) in HL,

Deleted: -

186

caudal-peduncle length 2.7 (3.6-4.8) in HL.

Deleted: -

187

Mouth small, terminal, oblique at about 45 degrees, upper-jaw length 4.3 (4.6-6.3) in HL; two

Deleted: -

188

pairs of enlarged canine teeth at front of upper jaw (two canines per side, anterior pair larger than

Deleted: -

189

posterior pair) and two pairs of enlarged canine teeth at front of lower jaw (two canines per side,

Deleted: -

190

anterior pair larger than posterior pair) fitting between upper pair when mouth is closed; teeth

Deleted: -

191

behind enlarged canines in a regular row of 10-15 caniniform to conical teeth in each quadrant;

Deleted: -

192

no posterior canine at corner of mouth. Upper preopercular margin free and smooth nearly to

Deleted: -

193

level of lower edge of orbit; lower margin free anterior to a vertical through anterior nostril. Gill

Deleted: -

194

rakers short, longest on first arch (at angle) about one-quarter length of longest gill filament.

Deleted: -

195

Nostrils small, in front of anterior edge of orbit. Head pores comprise two over maxilla, then two

Deleted: -

196

anterior to orbit, followed by a curving suborbital series of 6 pores in a single row up to rear mid-

Deleted: -

197

level of orbit.

Deleted: -

198

Scales thin, cycloid, and less than half as high on thorax as largest scales on flanks, still smaller
ventroanteriorly; head naked except for irregular rows of small partially embedded scales on nape except
midline; several progressively smaller scales on basal area of median fins and a mid-ventral scale projecting
posteriorly from pelvic-fin base. Scale rows above lateral line 4 and below

Deleted: -

199

lateral line 8; circumpeduncular scales 16. Lateral line continuous, nearly following contour of

Deleted: -

200

back to about 19th pored scale, below base of about 8th dorsal-fin soft ray, where deflected

Deleted: -

201 ventrally to a straight peduncular portion; anteriormost scales in holotype with 3 pores per scale,
202 after a few scales becoming two pores, and straight section with a single pore per scale; on all
203 (smaller) paratypes only a single pore per scale; last pored scale on caudal-fin base.

204 Origin of dorsal fin above anterior edge of second lateral-line scale; predorsal length 3.2 (3.3–
205 3.4) in SL; dorsal-fin base 1.5 (1.5–1.7) in SL; dorsal-fin spines progressively longer, first 5.9
206 (6.5–7.8) in HL; longest dorsal-fin spine 3.8 (3.6–3.9) in HL; longest dorsal-fin soft ray 2.5 (2.9–3.1) in HL;
207 origin of anal fin below base of last dorsal-fin spine; preanal length 2.1 (1.7–1.9) in SL; anal-fin
208 base 2.6 (2.5–2.9) in SL; first anal-fin spine short, 10.6 (13.3–16.4) in HL; second anal-fin spine 6.3
209 (5.4–5.9) in HL; third anal-fin spine 4.5 (4.1–4.7) in HL; longest anal-fin soft ray 3.0 (3.2–3.5) in HL;
210 caudal-fin length 1.9 (1.3–1.5) in HL; second or third pectoral-fin ray usually longest, 1.6 (1.7–
211 2.0) in HL; pelvic-fin spine short, 3.5 (3.4–4.3) in HL, pelvic-fin length 2.3 (2.4–2.5) in HL.

211 **Color in life.** (Figs. 2–6) Fresh TP specimens have a vermilion head and orangish-brown body,
212 grading to yellowish-cream ventrally. Head mostly uniformly colored, jaws paler, yellowish
213 below level of mandible, with a prominently reddish orange iris and a reddish orange opercular
214 flap with irregular indigo lines and dark purple in diffuse patches. Body with a cross-
215 hatched pattern of rows of scales with dark brown crescents with reddish borders on each scale,
216 grading to yellowish ventrally where spots are less conspicuous; upper abdominal area
217 underlying pectoral fin with opaque white underlying scales forming a conspicuous white patch.
218 Rear body with a large black patch covering end of caudal peduncle and extending over proximal

Deleted: ,

Deleted: -

Deleted: -

Commented [A1]: Mention which spine is the longest (numerically).

Eg., 5th dorsal-fin spine longest, 3.8 in HL.

Commented [A2]: As above

Deleted: -

Deleted: -

Deleted: -

Deleted: -

Deleted: -

Deleted: -

Commented [A3]: As above

Deleted: -

Deleted: -

Deleted: -

Deleted: -

Deleted: -

Deleted: -

Deleted: -

Formatted: Indent: Left: 1.34 cm, No bullets or numbering

Deleted: -

Deleted: and

219 half of caudal fin. Dorsal fin with a small black spot centered on first [interspinous](#) membrane and
 220 remaining dorsal-fin membranes with irregular yellowish bands and a blue marginal band along
 221 soft-dorsal-fin margin; small bright indigo spots at bases of anterior dorsal-fin spines; caudal-fin
 222 rays brownish orange fading to yellow distally, membranes translucent brown distally; anal fin
 223 yellow with bluish bands midfin and along margin; pectoral fins translucent, orange at base, axil
 224 with a small dark spot; pelvic fins with yellow band anteriorly.

225 Underwater, where red color is absorbed, head and body appear dusky purple to greenish, with
 226 dark cross-hatching from outlined scales; more prominent visible markings are pale lips, a large
 227 white patch over upper abdomen beneath pectoral fin, a pale dorsal-fin base with an expanded
 228 pale area just before black area on caudal peduncle, and a conspicuous black caudal blotch
 229 covering end of caudal peduncle and basal half of caudal fin.

230 IP fish pinkish grey dorsally grading to white on abdomen becoming yellowish posteriorly with a
 231 broad brick-red band running along lateral midline from snout to caudal peduncle, ending in a
 232 horizontal oblong black spot just above midline on caudal-fin base, iris bright red-orange in line
 233 with band, a distinct black crescent with indigo to purplish anterior margin on opercular flap;
 234 upper body with a less-prominent, thinner, reddish band running from upper snout to dorsal
 235 caudal peduncle, bands can form horizontal block segments when fish are disturbed. Dorsal fin
 236 with a large oblong black spot on basal two-thirds of fin, extending partially onto body scales,
 237 centered on last spine and first three rays, with most of upper margin of spot edged with yellow
 238 and white, forming a partial ocellus; a small dark spot in the pectoral-fin axil; [median](#) fin membranes
 239 translucent with brownish or faint purple-red rays. Juveniles (less than 20 mm SL) with similar

240 color pattern but black spots on mid-dorsal fin and caudal-fin base relatively larger and a more
241 rounded opercular-flap black spot.

242 **Color under fluorescence.** (Fig. 6) Entire body of TP male without fluorescent emission except
243 for slight yellow emission on pale patch beneath pectoral fin; dorsal, anal and pelvic-fin spines
244 and rays faint yellow. Entire body of IP fish bright red; eye dark without fluorescence except for
245 upper half to two-thirds of iris red; small, round opercular black spot; round to oblong black
246 spots at midpoint of dorsal fin and slightly above lateral line at base of caudal fin.

247
248 **Color in alcohol.** (Fig. 6) Head and body of TP male brownish with residual dark-centered scale rows and
249 black markings on first dorsal-fin membrane and rear caudal blotch persisting in preservative; IP
250 and juvenile individuals pale brownish with black marks on opercular flap, rounded spot on mid-
251 dorsal fin, and at end of mid-lateral body band on caudal-fin base.

252 **Etymology.** Named for Prof. Carlos Armando Sanchez Ortiz, of the Programa de Investigacion
253 para la Conservacion de la Fauna Arrecifal (PFA), Biologia Marina, Universidad Autonoma de
254 Baja California Sur (UABCS) in La Paz, Baja California Sur, Mexico, in recognition of his
255 contributions to the study of the marine communities of Pacific Mexico and who organized the
256 2022 expedition and collected the first specimen of the new species.

257 **Distribution.** The new species is presently known only from the Revillagigedo Archipelago: it
258 has been documented on Socorro Island by the underwater photographs of Kreg Martin in 2013
259 (Fig. 3) and from San Benedicto Island by our 2022 expedition. No other records exist in the
260 compendium of underwater photographs we have reviewed or in museum collections we have
261 examined.

262 **Habitat.** Specimens were only observed and collected at a specific site off the southern end of
 263 San Benedicto, just west of the popular El Canyon dive site at Caletilla Volteadura (Fig. 1). The
 264 site was a large, even plain, approximately 21–22 m deep, composed of volcanic gravel-rubble
 265 surrounded by lava boulders and with a few boulders dispersed in the plain amongst a dark
 266 bottom. Patches of white gravel were interspersed among the dark volcanic gravel-rubble areas.
 267 Juveniles and smaller IP fish were found generally just off the bottom around boulders and over
 268 lighter patches of gravel while larger IP and TP individuals were observed slightly higher in the
 269 water column around the boulders on the eastern edge of the plain.

Deleted: -

270 **DNA analysis.** (Fig. 7) The neighbor-joining phylogenetic tree based on the COI mtDNA sequences
 271 of a set of TEP *Halichoeres* species, following the Kimura two-parameter model
 272 (K2P) generated by BOLD (Barcode of Life Database), shows relatively low divergences
 273 between species within complexes and deep divergences between more distant sets of species.

Deleted: labrid species allied to *Halichoeres*

Formatted: Font: Italic

274 The position of *H. sanchezi* was recovered in a clade containing the two other
 275 members of the complex, i.e. *H. salmofasciatus* and *H. melanotis* (note that there are no
 276 sequences available for *H. malpelo*). The members of the complex are less than 3% divergent
 277 from each other: 2.4% between *H. sanchezi* and *H. melanotis*, 2.9% between *H. sanchezi* and *H.*
 278 *salmofasciatus*, and 2.1% between *H. melanotis* and *H. salmofasciatus* (all uncorrected pairwise distances).
 279 All other *Halichoeres* species are more than 13.5% different from the *H. melanotis* species
 280 complex.

Deleted: COI sequence

281 Interestingly, another endemic wrasse, *Halichoeres insularis* Allen & Robertson, 1992, was
 282 discovered on a prior expedition to the Revillagigedo Archipelago in 1991. That species diverges
 283 by 7.6% in mtDNA COI sequence from its widespread mainland sister species, *Halichoeres*

284 *dispilus* Gunther, 1864. The wide range in divergences of the putative endemic species in the
 285 Revillagigedo Archipelago, from 0.5% for *Thalassoma virens* Gilbert, 1890 (from *Thalassoma*
 286 *purpureum* Forsskal, 1775) up to 7.6% for *H. insularis*, makes it difficult to
 287 discern a pattern in phylogenetic age for the splitting of species in the region. Note the
 288 cytochrome-b sequence (GenBank accession number GU938863) for "*H. insularis*" used in Wainwright et al.
 (2018) is
 289 apparently a mislabeled sequence of *H. salmofasciatus*, leading to a mistaken assignment of *H.*
 290 *insularis* to the *H. melanotis* clade in the Bayesian timetree in their Fig. 2 and [in](#) Rocha, Pinheiro & Gasparini
 (2010): there were no tissues from Revillagigedo available to them at the time. An additional
 291 correction regarding the phylogenetic tree is that *Halichoeres burekae* Weaver & Rocha, 2007 as
 292 listed by Victor, Alfaro & Sorenson (2013) (GenBank accession number JN313704), is now identified as
Halichoeres
 293 *caudalis* (Poey, 1860) and newly obtained sequences for *H. burekae* are used in the tree here.
 294
 295 **Comparisons.** At the time of prior descriptions, there were few or no underwater photographs
 296 of various phases of the *H. melanotis* species complex to compare with, thus the table of color-
 297 pattern differences in Allen & Robertson (2002; Table 2) is no longer accurate. An updated table of color
 pattern differences is presented here in Table 2. Notably, Bessudo
 298 & Lefevre (2017), in their guide to the fishes of Malpelo, follow the 2002 table describing IP *H.*
malpelo as having neither the opercular-flap or caudal-peduncle spots and thus label their
 299 photographs of IP fish with the caudal spot as *H. salmofasciatus*, and those without as *H.*
malpelo (and listing both species for Malpelo Island). Recently, a set of additional underwater

Formatted: List Paragraph, Space Before: 0 pt

Formatted: List Paragraph, Space Before: 0 pt

Formatted: List Paragraph, Space Before: 0 pt

Formatted: List Paragraph, Space Before: 0 pt

Formatted: List Paragraph

Formatted: List Paragraph, Space Before: 0 pt

Formatted: List Paragraph, Space Before: 0 pt

Formatted: List Paragraph, Space Before: 0 pt

Formatted: List Paragraph, Space Before: 0 pt

Formatted: List Paragraph, Space Before: 0 pt

302 photographs have been taken of *H. salmofasciatus* on Cocos Island (Figs. 8 & 9), *H. malpelo*
303 on Malpelo Island (Figs 10 & 11), and *H. melanotis* from Panama and Baja California (Figs. 12-
304 14). These photographs greatly expand the known color variations for these species. *Halichoeres*
305 *sanchezi* is most similar in appearance to its southern island relatives. The IP adults of both *H.*
306 *salmofasciatus* and *H. malpelo* closely resemble *H. sanchezi*, except they lack the mid-dorsal-fin

Formatted: List Paragraph, Space Before: 0 pt

Formatted: List Paragraph, Space Before: 0 pt

Formatted: List Paragraph, Space Before: 0 pt

Formatted: List Paragraph, Space Before: 0 pt

Formatted: List Paragraph, Space Before: 0 pt

Formatted: List Paragraph

spot that is diagnostic of IP adult *H. sanchezi*. Allen & Robertson (2002) reported that the spot is only present on juvenile *H. salmofasciatus* below about 20 mm SL and a diagnostic photograph from Cocos Island shows that loss of the spot as individuals get larger (Fig. 8) (juveniles of *H. malpelo* have not been documented). The underwater photographs of the three *H. melanotis* complex species show wide variation in the color patterns of IP fishes with varying intensities of red from candy-stripe red to brown and the opercular-flap spot and the caudal-peduncle spot sometimes faded or absent.

The juveniles and IP of mainland *H. melanotis* are especially variable in appearance, with multiple different versions of juvenile color patterns (Fig. 12). One is the classic golden-yellow, black-striped juvenile (leading to the common name Golden Wrasse) as illustrated in Allen & Robertson (1992; 1994): it has been photographed frequently both in Panama and Baja California. The golden juveniles can have a mid-dorsal-fin spot on very small individuals, but it is quickly lost with age. In contrast, recent photographs by Allison Morgan Estape and Carlos Estape document quite different versions of juveniles and small IP fish in Panama and Baja California, coexisting with golden juveniles. Some are mostly black and white versions of the golden form, but others show dark bars with a variety of colors and a prominent colorful opercular flap with black and yellow and blue, similar to the flap of TP males; some of these small individuals can have a large round mid-dorsal spot, edged on the upper portion with yellow but not extending partially

Formatted: List Paragraph, Space Before: 0 pt

Formatted: List Paragraph, Space Before: 0 pt

Formatted: List Paragraph, Space Before: 0 pt

Formatted: List Paragraph, Space Before: 0 pt

Formatted: List Paragraph, Space Before: 0 pt

Formatted: List Paragraph

Formatted: List Paragraph, Space Before: 0 pt

Formatted: List Paragraph, Space Before: 0 pt

Formatted: List Paragraph, Space Before: 0 pt

Formatted: List Paragraph, Space Before: 0 pt

Formatted: List Paragraph, Space Before: 0 pt

Formatted: List Paragraph, Space Before: 0 pt

Formatted: List Paragraph, Space Before: 0 pt

Formatted: List Paragraph, Space Before: 0 pt

body scales as in juveniles of *H. sanchezi*. Another juvenile *H. melanotis* from the Sea of Cortez shows a different color pattern

325 but retains the opercular flap markings and has a large caudal-fin-base spot but no dorsal-fin spot

326 (Fig. 12). Both juvenile and IP phases can sometimes have a black spot on the membrane of the

327 first dorsal-fin spine, a feature of TP males of the *H. melanotis* complex. The significance of this

328 extreme variation in color patterns in this species remains to be clarified.

Formatted: List Paragraph, Space Before: 0 pt

Formatted: List Paragraph, Space Before: 0 pt

Formatted: List Paragraph, Space Before: 0 pt

Formatted: List Paragraph, Space Before: 0 pt

329 Larger IP adult *H. melanotis* also have a wide variety of color patterns, from pale salmon with
 330 the same black spots on the opercular flap and caudal-fin base of the other members of the
 331 complex to shades of grey, yellow, green, or brown with the black opercular-flap spot the only
 332 prominent marking (Fig. 13). Others show various degrees of a colorful barred pattern, some
 333 with a prominent "abdominal window" marking, a reddish purple or grey patch with conspicuous white
 334 streaks of myotomal fascia (this marking occurs in some other labrids, including *Halichoeres*
 335 *nebulosus* (Valenciennes, 1839) and some razorfishes). Larger IP adults can also show some blue
 336 lines and spots anterior to the opercular flap, but less prominent than on TP males.

337 The TP male of *H. sanchezi* shows the most divergence from relatives, most conspicuously the
 338 large black blotch covering the posterior caudal peduncle and the proximal half of the caudal fin.
 339 In contrast, the TP males of *H. salmofasciatus* (Fig. 9) and *H. malpelo* (Fig. 11) have black
 340 covering the posterior end of the caudal fin. They have a cross-hatched scale pattern on a mostly
 341 uniform greenish blue background with a pale abdomen, a yellowish wash on the snout, a bright
 342 red iris, and most have a pattern of reticulated blue lines and spots within the band behind the eye.
 343 The opercular flap ranges from a black oval to an inconspicuous bluish patch. Some photographs
 344 of *H. salmofasciatus* show a broad dusky midlateral band, broader than the red stripe of the IP,
 345 with only a dusky area on the rear caudal fin and these may include transitional stages from IP
 346 females to TP males. When disturbed, all adult members of the complex can display
 347 a barred pattern.

348
 349 In sharp contrast to *H. sanchezi*, the TP male of *H. melanotis* shows a wide range of color
 350 patterns (Fig. 14). Its most diagnostic feature is the absence of a dark caudal-fin marking as
 351 found on island species. The head and body can range from blue-green to yellowish to orange,
 352 the body can show cross-hatching with vertical blue lines or rows of spots on each scale or can

Deleted: develop

353 be uniform. The opercular flap is usually a distinct black vertical oval and a pale band extends
 354 from the chin across the lower operculum. All TP males have some degree of a complex pattern
 355 of small blue spots and lines on the head behind the eye. Some individuals with mostly IP
 356 patterns can also show these head patterns, perhaps including transitional stages. When the
 357 dorsal fin is raised, there is a small black spot on the first dorsal-fin membrane, as is found on TP
 358 *H. sanchezi*.

359

360 It is unclear what differentiates the IP and TP phases of *H. salmofasciatus* and *H. malpelo* from each other.
 361 In view of the variation in markings within these species, the taxonomic status of the two

362 species needs to be confirmed by additional documentation, as well as by molecular methods,
363 which can assist in evaluating populations for species-level differences.

364 **Remarks.** The joint expedition in November 2022 to the Revillagigedo Archipelago pioneered a
365 “gold standard” approach to documenting an inventory of the fish assemblage of an island by
366 combining diagnostic underwater photographs of the full set of species encountered , targeted collection of the
photographed subjects, on-deck
367 photographing of the fresh specimens, tissue sampling for molecular analysis, and preservation
368 of vouchers for museum collections. It brought together an international group of scientists (the
369 authors, Carlos Sanchez, D. Ross Robertson, Michelle Gaither, and Fernando Duarte), along with
370 a cadre of some of the most experienced tropical marine underwater photographers (in
371 alphabetical order): Alasdair Dunlap-Smith, Allison Morgan Estape, Carlos Estape, Jeffrey
372 Haines, Andres Hernandez, Ann S. Johnson, Keri Kenning, Serenity Mitchell, Ellie Place, Lee
373 Richter, and Sara Richter (Fig. 15). The expedition resulted in the most comprehensive

374 assessment of the fish fauna of a particular island to date, with more than 5,500 diagnostic underwater fish
 375 photographs of more than 152 species (Estep, 2023). The results are in preparation for
 376 publication and include a species list, a photographic inventory, a DNA-barcode coverage report
 377 and documentation of several new species to be described from the islands (Robertson et al., in
 378 prep).

378 A benefit of the comprehensive team approach to inventorying the fish fauna of an island is the
 379 opportunity for a detailed documentation of the discovery of a new species of fish. The novelty
 380 of this justifies a description of the process. Detailed videos and photographs of the collection
 381 dive, the process of locating, subduing and bagging the holotype, and the procedures following
 382 on board to process the specimens are archived at <https://doi.org/10.5281/zenodo.8384735> for videos and

<https://doi.org/10.5281/zenodo.8384765> for photographs.

383 In this case, an unknown species of wrasse was fleetingly observed and photographed by Kreg
 384 Martin in 2013 (Fig. 3). Both the TP and IP were observed at a single location, Punta Tosca on
 385 Socorro, at 20 m depth, on a REEF survey expedition led by Christy Semmens. Kreg Martin
 386 notes the fish were evasive and actively avoided divers and were especially difficult to
 387 photograph. At the time, the photographs were shown to author BCV and D. Ross Robertson and
 388 they concluded that it may represent an endemic species in the *H. melanotis* complex. However,
 389 no specimen was forthcoming and until our expedition, the status of the unknown species
 390 remained unresolved.

391 One of the priorities of the joint expedition was finding and documenting lesser-known species,
 392 especially those new to science. We did not encounter the unknown wrasse at Socorro or
 393 Clarion. However, on the last stop of the trip, at San Benedicto on 30 November 2022, the first
 394 dive of the morning was at the "El Canyon" dive site, to visit the shark-cleaning station. On the
 395 way back from the deep location, divers passed over a coarse gravel bed interspersed with small

396 rocks at about 20 m and Dr. Sanchez collected several small fishes, which included a single
 397 small IP of the new labrid species. On a subsequent dive targeting the same location, all
 398 divers focused on collecting, and a number of IP and juvenile wrasses were cornered and
 399 captured, not without difficulty since the fish sought refuge under rocks and then buried
 400 themselves in sand. Few TP males were observed, and one was cornered and lost. On a final
 401 dive, WBL managed to spear the previously lost TP male and WBL and BWF finally
 402 maneuvered the specimen into a bag and thus the holotype was firmly in hand (Fig. 16).

403 **Endemism.** The remoteness of the Revillagigedo Archipelago has certainly contributed to the
 404 development of endemism and the ratio of endemic species rivals that of any small oceanic
 405 island. Interestingly, the endemic fish species include both chaenopsids on the islands, two of the
 406 three known gobies, one of the two local *Thalassoma* species, *T. virens* (with a few records from
 407 Clipperton, and vagrants to Baja California in ENSO years (Victor et al., 2001), where they do
 408 not persist), and now two of the *Halichoeres* species. In comparison, the Galapagos Islands,
 409 Cocos Island, and Malpelo have no endemic *Thalassoma* species and fewer endemic *Halichoeres*
 410 species. They do match in having endemic chaenopsids and most of their gobies. A detailed
 411 exploration of Revillagigedo endemism will be reviewed in the upcoming inventory report of the
 412 fish fauna of the islands (Robertson et al., in prep.).

413 Conclusions

414 During an international effort to comprehensively inventory the ichthyofauna of the remote
 415 Revillagigedo Archipelago off the Pacific coast of Mexico, a new endemic species of wrasse
 416 (Labridae) was collected and documented by a team of underwater photographers collaborating with
 417 scientists. The new
 species, *H. sanchezi*, belongs to the *H. melanotis* species complex that is found

418 throughout the region, and it diverges 2.4% in the mtDNA COI sequence
 419 from its nearest relative, *H. melanotis* from Panama, and 2.9% from *H. salmofasciatus* from
 420 Cocos Island, off Costa Rica. The juveniles and IP of the new species closely resemble
 421 those of *H. salmofasciatus* and *H. malpelo* from Malpelo Island off Colombia, while the TP has a color pattern
 distinct from other relatives, most notably having a
 422 prominent black patch on the caudal peduncle and base of the caudal fin. The new species adds
 423 to the list of endemic fish species for the isolated archipelago and is an interesting case of island
 424 endemism in the region.

425 **Acknowledgements.** We are especially grateful to Carlos Sanchez (UABCS) for initiating,
 426 arranging, facilitating, and leading the 2022 expedition, as well as creating an exceptionally
 427 friendly collegial atmosphere. Fernando Duarte, also from UABCS, is appreciated for his able
 428 assistance. D. Ross Robertson of the Smithsonian Tropical Research Institute provided
 429 unparalleled taxonomic expertise and his guide to SFTEP was the indispensable reference
 430 database to which to refer. Allison Morgan Estape was instrumental in organizing the logistics of
 431 getting so many people and their equipment in the same place at the same time. We are all
 432 indebted to Dora Sierra, the owner of the vessel Quino el Guardian, and the cooperative and
 433 patient crew and dive masters who made the trip possible (and safe). We thank William Bensted-
 434 Smith, Sandra Bessudo, Allison Morgan Estape, Carlos Estape, Jeff Haines, Andres Hernandez, Kreg Martin,
 435 Ellie Place, D. Ross Robertson, and Sara Richter for permission to use their photographs and
 436 Sofia Lopez, Christy Semmens, and Lourdes Vasquez-Yeomans for facilitating access to photographs and
 other assistance. Finally, the group of
 437 enthusiastic underwater photographers: Alasdair Dunlap-Smith, Allison Morgan Estape, Carlos
 438 Estape, Jeffrey Haines, Andres Hernandez, Ann S. Johnson, Keri Kenning, Serenity Mitchell, Ellie
 439 Place, Lee Richter, and Sara Richter, who provided much of the human energy for the project,

440 need to be acknowledged for their unparalleled skill in finding fishes, creating superbly
441 composed photographs (usually while upside down and rolling), and being endlessly upbeat,
442 humorous, and passionate about fishes and marine biology.

443 References

444 Allen GR, Robertson DR. 1992. Deux nouvelles especes de Girelles (Labridae: *Halichoeres*) du
445 Pacifique oriental tropical. *Revue francaise d'aquariologie herpetologie* 19(1-2):47-52.

446 Allen GR, Robertson DR. 1994. *Fishes of the tropical eastern Pacific*. University of Hawaii
447 Press.

448 Allen GR, Robertson DR. 2002. *Halichoeres salmofasciatus*, a New Species of Wrasse
449 (Labridae) From Isla Del Coco, Tropical Eastern Pacific. *Aqua, Journal of Ichthyology and*
450 *Aquatic Biology* 5(2):65-72.

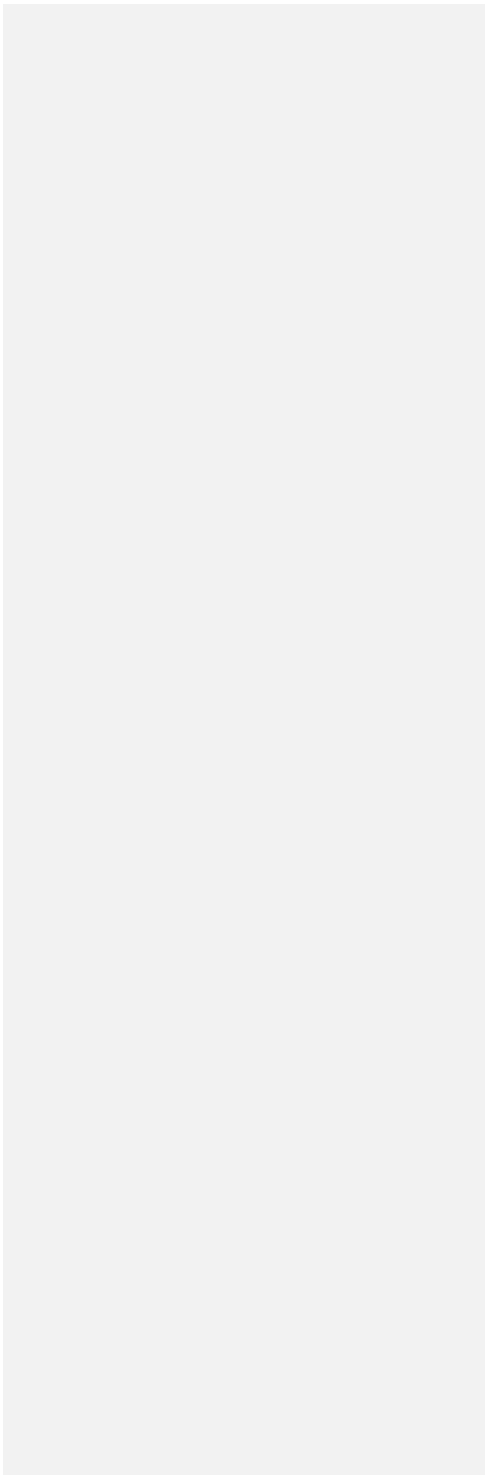
451 Bessudo S, Lefevre Y. 2017. *Guia de Peces Isla Malpelo Santuario de Fauna y Flora,*
452 *Colombia, Pacifico Oriental Tropical*. Fundacion Malpelo y Otros Ecosistemas Marinos.

453 Del Moral-Flores LF, Gracian-Negrete JM, Guzman-Camacho AF. 2016. Fishes of Archipelago of
Revillagigedo Islands: a systematic and biogeographic update. *BIOCYT Biologia, Ciencia y Tecnologia*,
9(34):596-619. <https://doi.org/10.22201/fesi.20072082.2016.9.75910>

454 Estape, AM. 2023. Documenting Reef-Fish Diversity in the Revillagigedo Archipelago, Pacific Mexico,
November 2022. Available at <https://doi.org/10.5281/zenodo.8146183> (accessed December 7, 2023).
455

Fourriere M, Reyes-Bonilla H, Ayala-Bocos A, Ketchum J, Chavez-Comparan JC. 2016. Checklist and analysis of
completeness of the reef fish fauna of the Revillagigedo Archipelago, Mexico. *Zootaxa* 4150(4):436-466.
<https://doi.org/10.11646/zootaxa.4150.4.4>

456 Ratnasingham S, Hebert PDN. 2007. BOLD: The Barcode of Life Data System
457 (www.barcodinglife.org). *Molecular Ecology Notes* 7:355-364.



459 Robertson DR, Allen GR. 2015. Shorefishes of the Tropical Eastern Pacific: online information
 system. Version 2.0.
 Smithsonian Tropical Research Institute, Balboa, Panamá. Available at <https://biogeodb.stri.si.edu/sfiep/en/pages>
 (accessed October 5, 2023).
 460

461 Rocha LA, Pinheiro HT, Gasparini JL. 2010. Description of *Halichoeres rubrovirens*, a new
 462 species of wrasse (Labridae: Perciformes) from the Trinidad and Martin Vaz Island group,
 463 southeastern Brazil, with a preliminary mtDNA molecular phylogeny of the New World
 464 *Halichoeres*. *Zootaxa* 2422:22-30. <https://doi.org/10.11646/zootaxa.2422.1.2>

465 Victor BC, Wellington GM, Robertson DR, Ruttenberg BI. 2001. The effect of the El Nino-
 466 Southern Oscillation event on the distribution of reef-associated labrid fishes in the eastern
 467 Pacific Ocean. *Bulletin of Marine Science* 69:279-288.

468 Victor BC, Alfaro ME, Sorenson L. 2013. Rediscovery of *Sagittalarva inornata* n. gen., n. comb.
 469 (Gilbert, 1890) (Perciformes: Labridae), a long-lost deepwater fish from the eastern Pacific
 470 Ocean: a case study of a forensic approach to taxonomy using DNA barcoding. *Zootaxa*
 471 3669(4):551-570. <https://doi.org/10.11646/zootaxa.3669.4.8>

472 Victor BC. 2016. Two new species in the spike-fin fairy-wrasse species complex (Teleostei: Labridae:
Cirrhitilabrus) from the Indian Ocean. *Journal of the Ocean Science Foundation*, 23:21–50.
<https://doi.org/10.5281/zenodo.163217>

473 Wainwright PC, Santini F, Bellwood DR, Robertson DR, Rocha LA, Alfaro ME. 2018.
 474 Phylogenetics and geography of speciation in New World *Halichoeres* wrasses. *Molecular*
 475 *Phylogenetics and Evolution* 121:35-45. <https://doi.org/10.1016/j.ympev.2017.12.028>

481